Jet Propulsion Laboratory
California Institute of Technology

Other Uses of the Adjoint

Ichiro Fukumori
Jet Propulsion Laboratory, Caltech

ECCO Summer School 2019

Identifying Causation

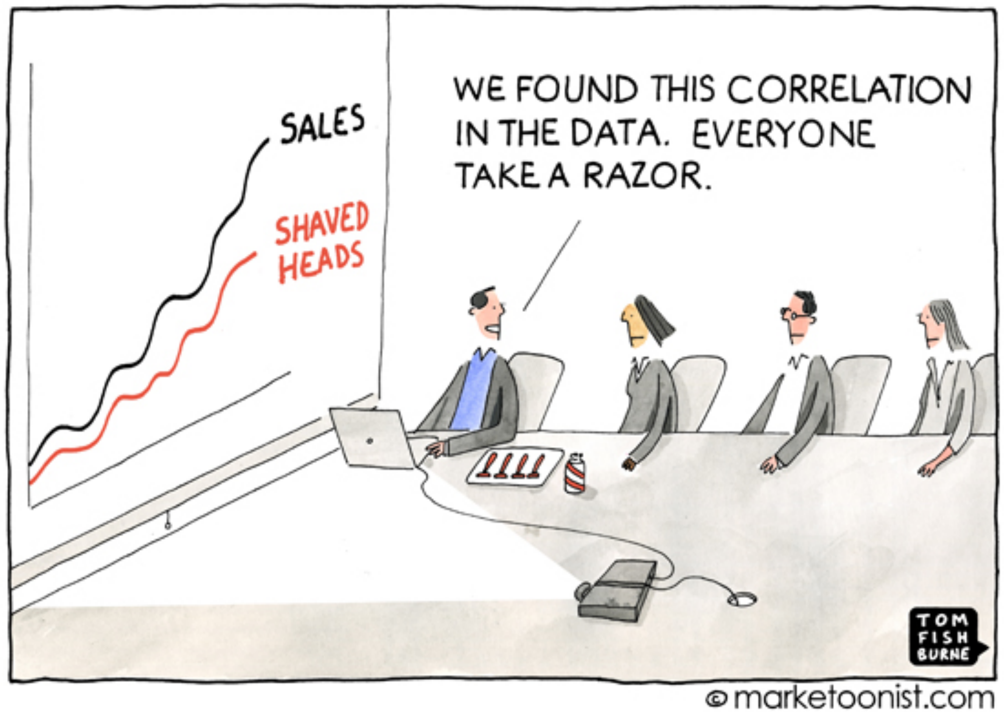

Correlation does not imply causation,
but adjoints do.

Physical Significance of Adjoint

Adjoints provide an efficient means to compute sensitivity of the model to controls in the past.

quantity of interest

$$\frac{\partial F\left[\mathbf{x}(t+N)\right]}{\partial \mathbf{u}(t)} = \frac{\partial \mathbf{x}(t+1)}{\partial \mathbf{u}(t)} \frac{\partial \mathbf{x}(t+2)}{\partial \mathbf{x}(t+1)} \frac{\partial \mathbf{x}(t+3)}{\partial \mathbf{x}(t+2)} \cdots \frac{\partial F\left[\mathbf{x}(t+N)\right]}{\partial \mathbf{x}(t+N)}$$

$$= \mathbf{G}^T \left(\mathbf{A}^T\right)^{N-1} \frac{\partial F\left[\mathbf{x}(t+N)\right]}{\partial \mathbf{x}(t+N)}$$

$$\mathbf{x}(t) = \mathbf{A}\mathbf{x}(t-1) + \mathbf{G}\mathbf{u}(t-1)$$

e.g.,

$$F\left[\mathbf{x}(t+N)\right] \equiv a x_i(t+N) + b x_j(t+N)$$

$$\partial F\left[\mathbf{x}(t+N)\right] / \partial \mathbf{x}(t+N) = \left(\cdots \quad \overset{i}{a} \quad \cdots \quad \overset{j}{b} \quad \cdots\right)^T$$

Identifying Causal Mechanisms

Adjoint gradients can help identify causal mechanisms.

Adjoint Gradient Decomposition/Reconstruction/Convolution

$$\delta J(t) \approx \underbrace{\sum_i \sum_{\mathbf{r}} \sum_{\Delta t}} \frac{\partial J(t)}{\partial u_i(\mathbf{r}, t-\Delta t)} \delta u_i(\mathbf{r}, t-\Delta t)$$

$$\approx \sum_i \sum_{\mathbf{r}} \sum_{\Delta t} \frac{\partial J(T)}{\partial u_i(\mathbf{r}, T-\Delta t)} \delta u_i(\mathbf{r}, t-\Delta t)$$

$$\approx \sum_i \sum_{\mathbf{r}} \sum_{\Delta t} \frac{\partial J}{\partial u_i}(\Delta t)\ \delta u_i(\mathbf{r}, t-\Delta t)$$

quantity of interest

forcing type, location, lag

forcing

Sensitivity of J of particular time T

gradient as a function of lag Δt

The largest terms on the right-hand-side identify the cause of J .

Example: Cause of Arctic-wide OBP Oscillation

Bottom pressure varies near-uniformly
across the deep Arctic basins

OBP time-series data

±5 cm

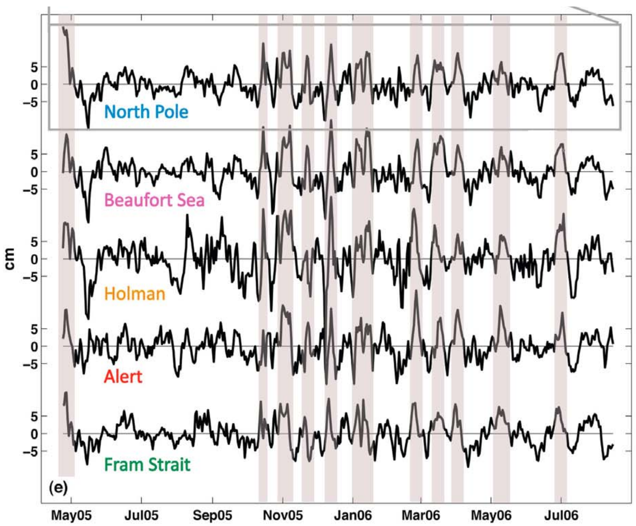

May 05

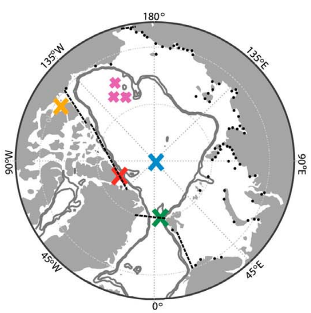

Jul 06

[*Peralta-Ferriz et al., 2011*]

GRACE

ECCO V4

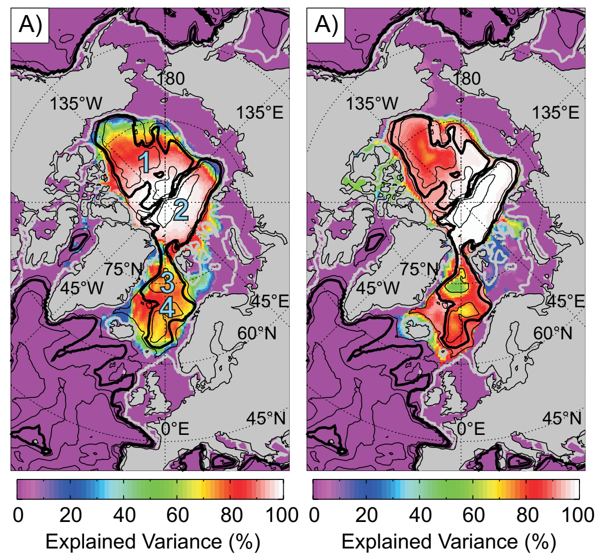

Spatial coherence (explained variance of North Pole OBP by OBP elsewhere.)

$$1-\frac{\mathrm{var}\left(p-p_{NP}\right)}{\mathrm{var}\left(p_{NP}\right)}$$

Arctic mean

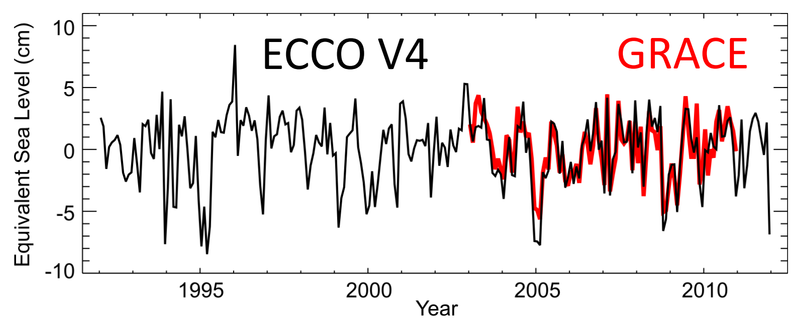

[*Fukumori et al., 2015*]

Example: Cause of Arctic-wide OBP Oscillation

Cause as a function of forcing, location & lag

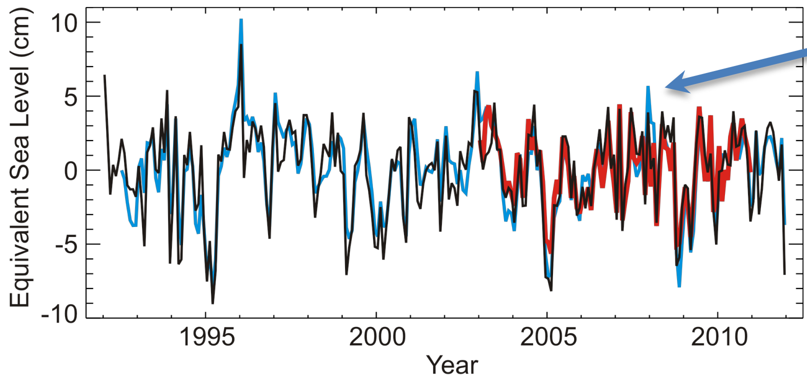

convolution with only wind

$$\delta J(t) \approx \sum_i \sum_{\mathbf{r}} \sum_{\Delta t} \frac{\partial J}{\partial u_i}(\Delta t)\, \delta u_i(\mathbf{r}, t-\Delta t)$$

vs location $\mathbf{r}$

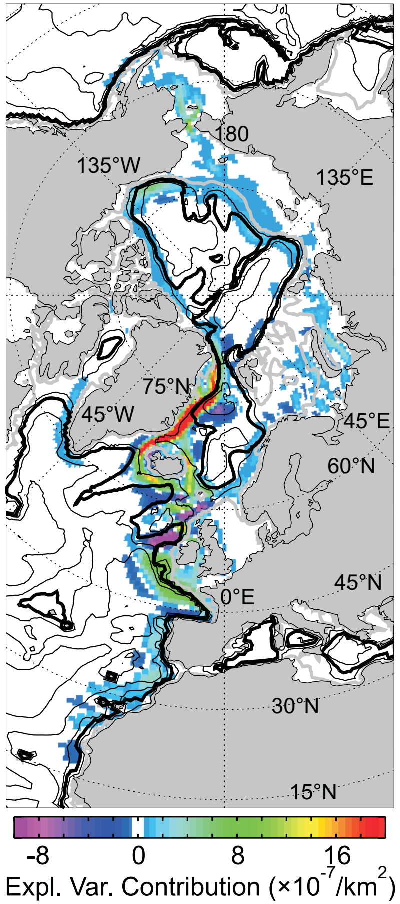

Explained variance as a function of forcing type, location & lag.

$$1 - \frac{\mathrm{var}\left(\delta J - \sum_i \sum_{\Delta t} \frac{\partial J}{\partial u_i(\mathbf{r}, \Delta t)} \delta u_i(\mathbf{r}, t-\Delta t)\right)}{\mathrm{var}(\delta J)}$$

vs lag Δt

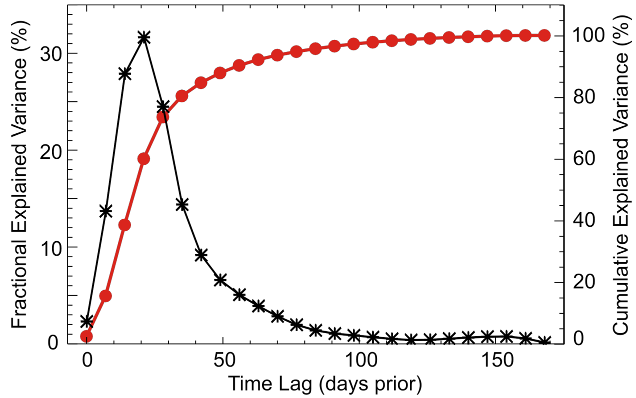

Example: Cause of Arctic-wide OBP Oscillation

Mechanism of Arctic OBP variation

Sensitivity to along-shore wind

$$\frac{\partial J}{\partial u_i(\mathbf{r}, \text{4-wks})}$$

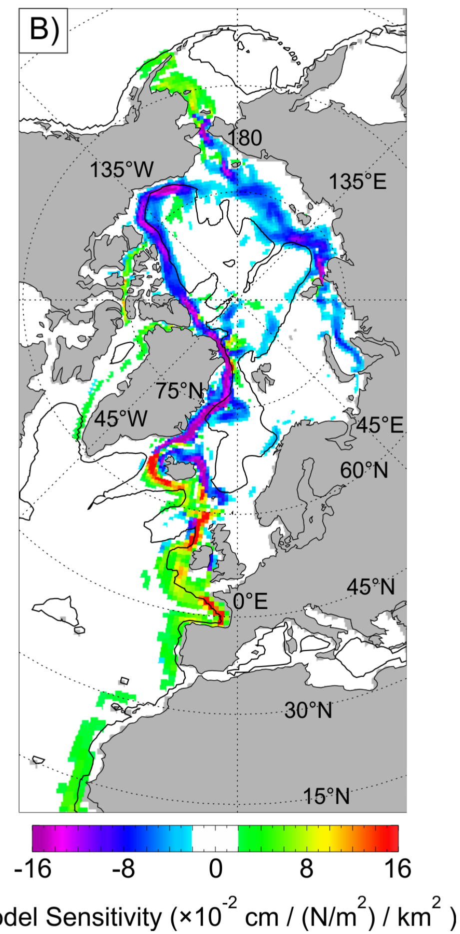

Results implicate bifurcating coastally-trapped waves

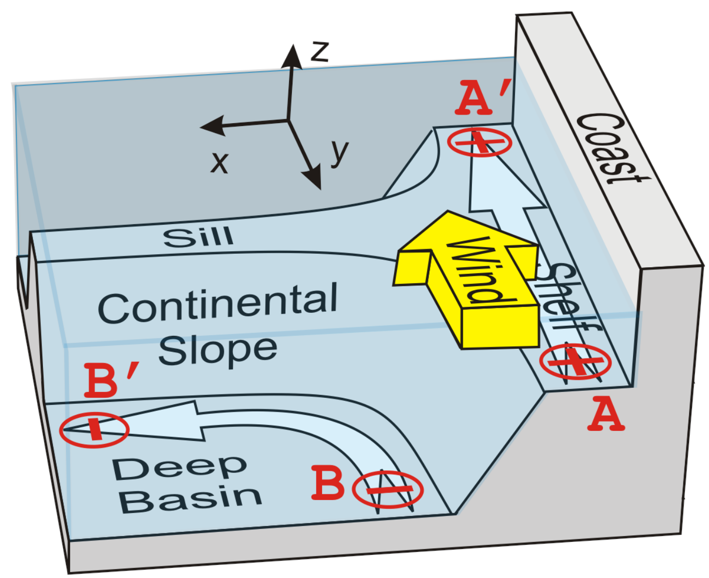

Example: Cause of Arctic-wide OBP Oscillation

OBP response to wind perturbation

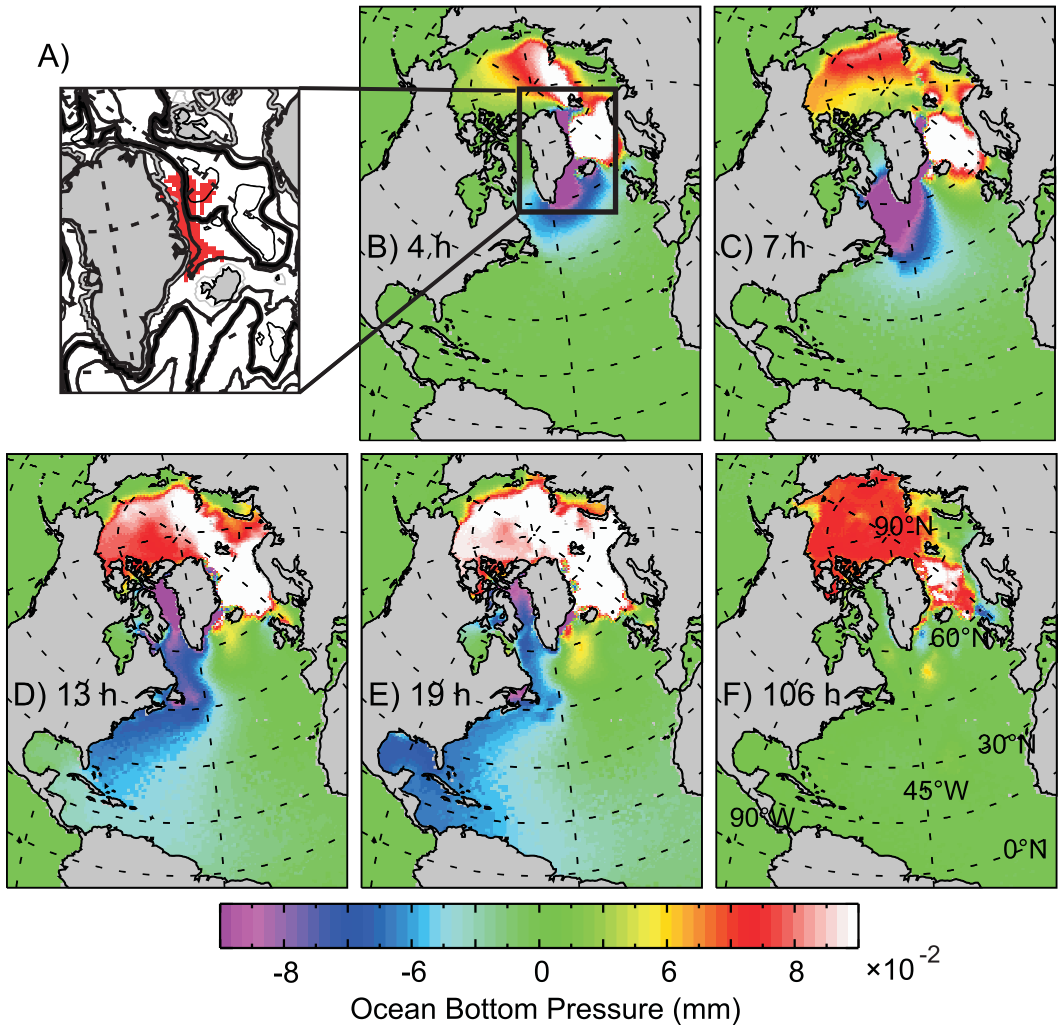

Example: Cause of Arctic-wide OBP Oscillation

Adjoint decomposition vs Correlation

Explained variance by location of forcing

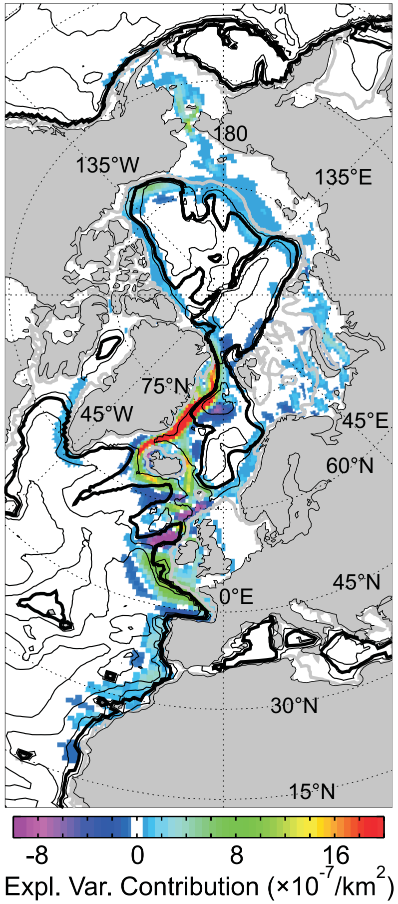

[*Fukumori et al., 2015*]

OBP regression with atmospheric wind & pressure

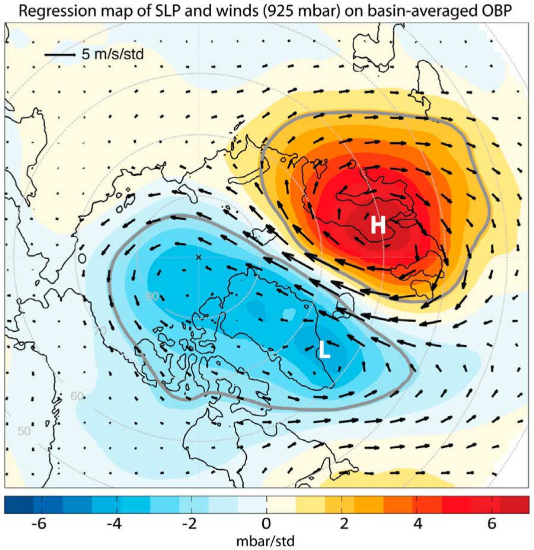

[*Peralta-Ferriz et al., 2011*]

Other Examples of Adjoint Decomposition

- Near-uniform sea level fluctuations of the Mediterranean Sea [*Fukumori et al., 2007*]

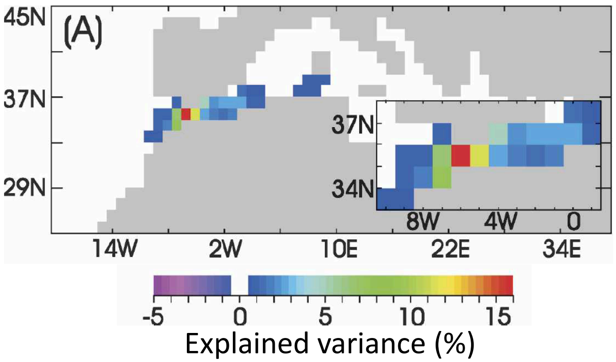

Zonal winds through Gibraltar Strait control sea level of the entire Mediterranean.

- Forcings driving Atlantic Meridional Overturning Circulation at 36S [*Smith & Heimbach, 2019*]

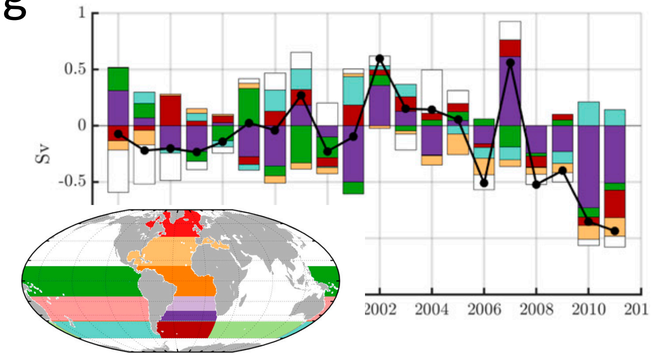

Local zonal winds dominate but remote forcing is not negligible.

- Other examples;

Zhang et al., (2011, 2012); Czeschel et al., (2012);
Wilson et al. (2013); Verdy et al. (2014); Pillar et al., (2016)

Origin, Pathway and Fate of a Water Mass

Adjoint passive tracers track where the tracer-tagged water comes from.

Forward evolution of a passive tracer describes where the tracer-tagged water goes to:

$$\partial \mathbf{c} / \partial t = -\mathbf{u} \cdot \nabla \mathbf{c} + \nabla \cdot \left(\kappa \nabla \mathbf{c} \right)$$

Backward evolution of an adjoint passive tracer describes where the adjoint tracer-tagged water comes from:

$$J = \int \mathbf{c}(T)\, dS \qquad \partial J / \partial \mathbf{c}(T - t) \equiv \mathbf{c}^*(t)$$

$$-\partial \mathbf{c}^* / \partial t = +\mathbf{u} \cdot \nabla \mathbf{c}^* + \nabla \cdot \left(\kappa \nabla \mathbf{c}^* \right)$$

$$\partial J / \partial \mathbf{c}(T) \equiv \mathbf{c}^*(0) = \delta(S)$$

[*Fukumori et al., 2004*]

Origin and fate of Nino3 water

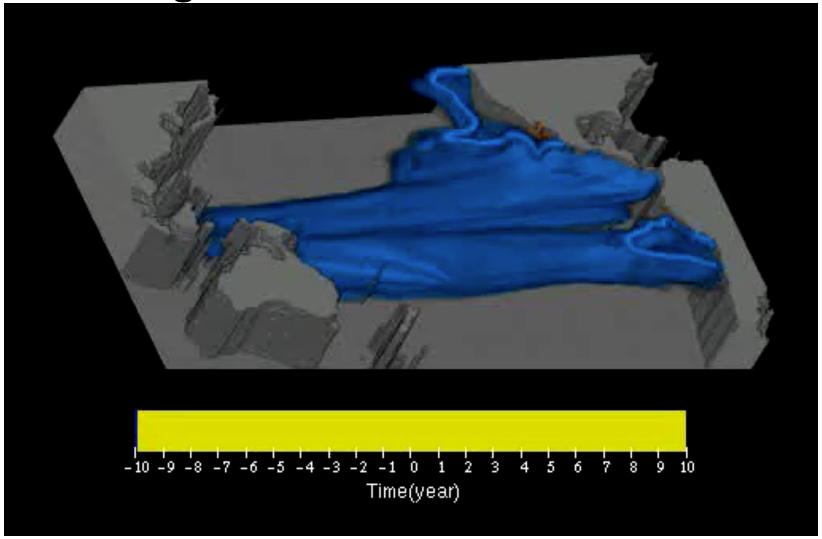

References

Czeschel, L., C. Eden, and R. J. Greatbatch, 2012: On the Driving Mechanism of the Annual Cycle of the Florida Current Transport. *J Phys Oceanogr*, **42,** 824-839, doi:10.1175/jpo-d-11-0109.1.

Fukumori, I., T. Lee, B. Cheng, and D. Menemenlis, 2004: The origin, pathway, and destination of Nino-3 water estimated by a simulated passive tracer and its adjoint. *J Phys Oceanogr*, **34,** 582-604, doi:10.1175/2515.1.

Fukumori, I., D. Menemenlis, and T. Lee, 2007: A near-uniform basin-wide sea level fluctuation of the Mediterranean Sea. *J Phys Oceanogr*, **37,** 338-358, doi:10.1175/Jpo3016.1

Fukumori, I., O. Wang, W. Llovel, I. Fenty, and G. Forget, 2015: A near-uniform fluctuation of ocean bottom pressure and sea level across the deep ocean basins of the Arctic Ocean and the Nordic Seas. *Prog Oceanogr*, **134,** 152-172, doi:10.1016/j.pocean.2015.01.013.

Peralta-Ferriz, C., J. H. Morison, J. M. Wallace, and J. L. Zhang, 2011: A basin-coherent mode of sub-monthly variability in Arctic Ocean bottom pressure. *Geophys Res Lett*, **38**, doi:10.1029/2011gl048142.

Pillar, H. R., P. Heimbach, H. L. Johnson, and D. P. Marshall, 2016: Dynamical attribution of recent variability in Atlantic overturning. *Journal of Climate*, **29,** 3339-3352, doi:10.1175/JCLI-D-15-0727.1.

Smith, T., and P. Heimbach, 2019: Atmospheric Origins of Variability in the South Atlantic Meridional Overturning Circulation. *Journal of Climate*, **32,** 1483-1500, doi:10.1175/jcli-d-18-0311.1.

Verdy, A., M. R. Mazloff, B. D. Cornuelle, and S. Y. Kim, 2014: Wind-driven sea level variability on the California coast: An adjoint sensitivity analysis. *J Phys Oceanogr*, **44,** 297-318, doi:10.1175/JPO-D-13-018.1.

Wilson, C., K. J. Horsburgh, J. Williams, J. Flowerdew, and L. Zanna, 2013: Tide-surge adjoint modeling: A new technique to understand forecast uncertainty. *J Geophys Res-Oceans*, **118,** 5092-5108, doi:10.1002/jgrc.20364.

Zhang, X. B., B. Cornuelle, and D. Roemmich, 2011: Adjoint Sensitivity of the Nino-3 Surface Temperature to Wind Forcing. *Journal of Climate*, **24,** 4480-4493, 10.1175/2011jcli3917.1.

Zhang, X. B., B. Cornuelle, and D. Roemmich, 2012: Sensitivity of western boundary transport at the mean North Equatorial Current bifurcation latitude to wind forcing. *J Phys Oceanogr*, **42,** 2056-2072, doi:10.1175/jpo-d-11-0229.1

Jet Propulsion Laboratory
California Institute of Technology